Organic Process Research & Development

Article

pubs.acs.org/OPRD

Kinetic and Scale-up Investigations of a Michael Addition in Microreactors

Sebastian Schwolow,[†] Birgit Heikenwälder,[†] Lahbib Abahmane,[‡] Norbert Kockmann,[§] and Thorsten Röder*[,†]

[†]Institute of Chemical Process Engineering, Mannheim University of Applied Sciences, Paul-Wittsack-Str. 10, 68163 Mannheim, Germany

[‡]3M ESK Ceramics GmbH & Co. KG, Max-Schaidhauf-Str. 25, 87437 Kempten, Germany

[§]Biochemical and Chemical Engineering, Equipment Design, TU Dortmund, Emil-Figge-Straße 68, 44227 Dortmund, Germany

Supporting Information

ABSTRACT: Microreactors are an efficient tool for process development and intensification. However, the scale-up from lab studies to small-scale commercial production is challenging, since a change in the channel dimensions requires good knowledge of heat and mass transfer phenomena. In this work, complete process development for an exothermic Michael addition is presented. In a systematic scale-up approach, kinetic studies and experimental characterization of the employed reactors provide key parameters for detailed reactor modelling. The residence time distribution, reactant mixing, and removal of reaction heat are taken into account. It is exemplarily shown how preliminary experiments can be the basis for the prediction of scale-up effects and the development of a continuous production process. Plug flow behavior and short mixing times could be confirmed for all investigated flow reactors. Furthermore, interactions of reaction kinetics and the formation of hot spots in the reactor channel were investigated. For the examined reaction, the simulations predicted the product yield under production conditions in good accuracy.

INTRODUCTION

The main advantages of microreactors are rapid mixing and excellent temperature control of chemical reactions.[1,2] Both processes strongly depend on the reactor dimensions. In microchannels, efficient mixing results from a high local energy dissipation rate and short diffusion paths.[3] The speed of heat removal in a microreactor not only benefits from the short length scale for heat transfer, but also from a high heat transfer coefficient in laminar flow at small channel diameters. During scale-up to commercial production, the outstanding performance of microreactors is often maintained by numbering up with massive parallelization. Since the scale-up by multiplication results in high equipment costs and problems such as flow maldistribution,[4,5] this concept has low practical value. Therefore, the scale-up considerations described in this paper focus on the transfer to larger equipment scale, which requires good investigation of the interaction of transport and kinetic phenomena. In the case of a fast and exothermic reaction, especially the temperature control is a crucial aspect, since parametric sensitivity can cause problems in terms of reactor stability. The scale-up can be critical since an increase of the channel diameter of 1 order of magnitude can increase the characteristic times for mixing and heat transfer to a much larger extent.[6] In this paper, we discuss different aspects of the development of a continuous process for an exothermic reaction, exemplarily demonstrated with the synthesis of 3-piperidino propionic acid ethyl ester by a Michael addition.

For the addition of secondary amines to α,β-unsaturated carbonyl compounds and nitriles, Löwe and Hessel[7] showed a significantly higher productivity in microstructured flow reactors compared to the traditional batch process. Due to superior heat removal in microreactors, the exothermic Michael additions could be carried out without any solvent. In consequence, the reaction time was decreased from 25 h in semibatch operations to only a few minutes in microreactors. This example clearly demonstrates the use of microreactors enabling safe operation of fast exothermic solvent-free reactions. The decrease in reaction time due to the enhanced heat removal as well as the increasing interest in solvent-free reactions as subject of green synthesis could be important drivers to consider the application of a flow reactor in a small-scale production process.[8]

In this paper, a general approach for process development is proposed: First, kinetic data of the reaction are obtained by a series of experiments using a microreactor with small internal volume of a few microliters. Analysis of reactor characteristics (Reactor Characteristics Section) allows for confirmation of the assumption of an ideal, nearly isothermal plug flow reactor behavior. On this basis, experimental data can be used for fitting the results to a kinetic model. In a subsequent step, the scale-up from the microscaled reactor to a production reactor has to be considered. Increasing the channel diameter and changing flow rates strongly influences the mixing performance, residence time distribution, and the efficiency in heat transfer. Reliable parameters for the calculation of these effects can be obtained by experimental characterization of the production

Special Issue: Continuous Processes 14

Received: August 28, 2014
Published: October 14, 2014

   dx.doi.org/10.1021/op5002758 | Org. Process Res. Dev. 2014, 18, 1535−1544

reactor (Scale-up of reactor concept Section). Simulations based on the combination of these parameters together with the kinetic model enable the prediction of product yield in the production reactor. In a final step, lab experiments close to production conditions should be performed in order to verify the scale-up approach.

MATERIALS AND METHODS

Reaction. The synthesis of 3-piperidinopropionic acid ethyl ester by a Michael addition (Scheme 1) was realized with nearly

Scheme 1. Synthesis of 3-piperidinopropionic acid ethyl ester

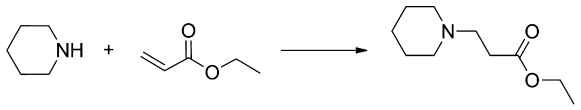

neat reactants at temperatures between 30 and 70 °C. However, a defined amount of 1-hexanol (11.5 wt %), used as internal standard for analytics, was added to the reactant ethyl acrylate. The resulting initial concentration of ethyl acrylate in the reactant mixture, including both reactant streams, had a final concentration of 4 mol/L. Since the influence of water on the reaction was examined, water was premixed with piperidine. Additionally, 1-butanol was added as a second internal standard. The amount of 1-butanol was chosen in order to adjust the initial concentration of piperidine for experiments with equal flow rates, e.g., 4.4 mol/L for a molar ratio of 1.1. An effective quench of the reaction at the outlet of the reactors was realized by mixing with a solution of acetic acid in methanol (11 vol. %). Thus, the reaction is terminated at a specified location, and the reaction time can be calculated by the flow rate and internal reactor volume between quench and reactant mixer.

Experimental Setup. For steady-state kinetic studies, lab experiments have been performed with a flexible microreactor setup (Figure 1). It was aimed to operate at low flow rates, but in a wide range of mean residence times in order to cover the whole reaction progress. Thus, different reaction channel dimensions had to be chosen. For short reaction times, a 1/16 in. stainless steel capillary reactor with an inner diameter of 250 μm (tube length 0.5 m) was used. Larger reactor volume was realized with a 1/16 in. capillary of equal length and 750 μm inner diameter. Both residence time modules were constructed as helical coils, with an alternating change in the direction of curvature, which is repeated every two coils (Figure 1b).

Reactants are preheated in 1/16 in. capillaries (inner diameter 1000 μm, tube length 2 m) and mixed in a slit interdigital mixer (SIMM-V2, Fraunhofer ICT-IMM, Mainz, Germany). Temperature control of preheating, mixing, and residence time modules was achieved in a bath thermostat. In order to stop the reaction precisely after an adjusted residence time, a T-junction (inner diameter 500 μm) was used to quench the product continuously with acetic acid solution in a volume ratio of 10:1. Quenched samples were collected with an automatic sampler (Autosam, HiTec Zang GmbH, Germany) in 5 mL vials. The continuous feed and quench streams are supplied by three continuous syringe pumps (Syrdos 2, HiTec Zang GmbH) with 1 mL glass syringes. By using a laboratory automation system (LabBox and LabVision Software, HiTec Zang GmbH), a series of experiments were realized with automated procedures including sampling, temperature, and flow rate settings. All samples were analyzed on an Agilent 7820 gas chromatograph equipped with a HP-5 column (30 m × 0.32 mm × 0.25 μm, Agilent) and a flame ionization detector. The inlet temperature was 275 °C, the inlet pressure, 50 kPa, and the split ratio, 100:1. An injection volume of 0.5 μL was used in the automatic liquid sampler. The oven temperature of 60 °C was kept constant for 2 min and then increased to 200 °C with a ramp of 20 K/min.

Determination of the Mixing Performance. To characterize the mixing process, an experimental approach with competitive reactions was taken. The chosen test reaction, a diazo coupling, is one of several mixing sensitive test reactions that were described by Baldyga, Bourne, and co-workers,[9−11] often also called fourth Bourne test reaction. In a first, quasi-instantaneous reaction of 1-naphthol (A) and diazotized sulphanilic acid (B), isomeric monoazo dyes 2-[(4′-sulphophenyl)azo]-1-naphthol (o-R) and 4-[(4′-sulphophenyl)azo]-1-naphthol (p-R) are formed (1a−1b). Subsequently, their secondary couplings produce one bisazo dye (S), in a fast, but comparatively slower reaction (1c−1d).

$$A + B \rightarrow o\text{-}R \quad (1a)$$

$$A + B \rightarrow p\text{-}R \quad (1b)$$

$$o\text{-}R + B \rightarrow S \quad (1c)$$

$$p\text{-}R + B \rightarrow S \quad (1d)$$

For the detailed reaction scheme and kinetic aspects, see Baldyga et al.[11] and Bourne et al.[9] This experimental approach is focusing on the ratio of the characteristic times for mixing and reaction. If the mixing time is significantly shorter than the reaction time, it can be assumed that the reaction takes place in

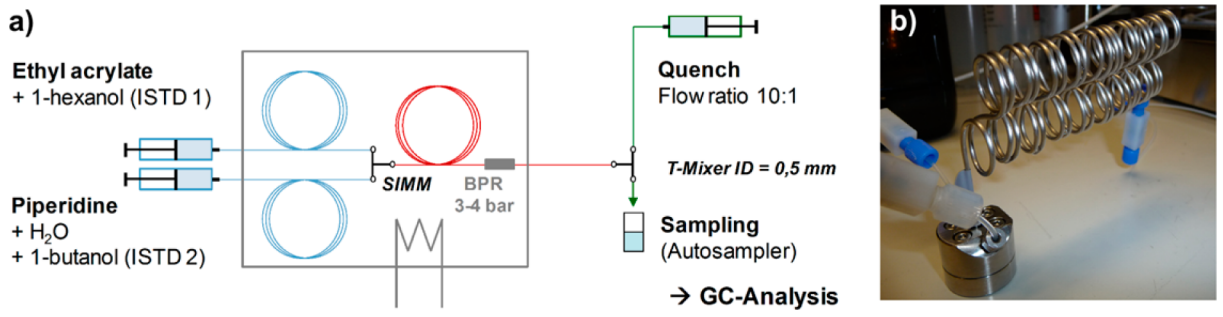

Figure 1. Microreactor setup for kinetic experiments (a), employing a microreactor with a coiled stainless steel capillary, connected to a slit interdigital micromixer (b).

dx.doi.org/10.1021/op5002758 | Org. Process Res. Dev. 2014, 18, 1535−1544

a homogeneous concentration field. In this case, selectivity is determined only by chemical kinetics. The limiting reactant B is consumed by the faster primary coupling, and the yield of product S approaches zero. In contrast, if the reaction is fast compared to mixing, the reaction takes place at the interfacial region of segregated fluid lamellae. After the immediate reaction of A and B, this region contains an excess of species o-R/p-R. Subsequently, reactants o-R and p-R continue to diffuse toward the region with a local overconcentration of reactant B, where (in the absence of species A) the slower reaction can proceed. As a result, a detectable yield of product S will be achieved, depending on the degree of segregation. Based on a closed material balance and no further byproduct formation, the yield of the bisazo dye S in relation to the initial concentration of B ($c_{B,0}$) can be defined as

$$Y_S = \frac{2c_S}{c_{B,0}} = \frac{2c_S}{c_{o\text{-}R} + c_{p\text{-}R} + 2c_S} \quad (2)$$

where $c_{o\text{-}R}$, $c_{p\text{-}R}$, and c_S are the concentrations of the products o-R, p-R, and S. The initial solution containing the diazonium salt was prepared by diazotization of 3 mol/m^3 sulphanilic acid with sodium nitrite and hydrochloric acid. Excess nitrite was eliminated by adding sulphamic acid. 3.6 mol/m^3 of 1-naphthol was dissolved in water by stirring and heating the solution. This stream was buffered using 222.2 mol/m^3 each of sodium carbonate and bicarbonate in order to obtain a pH of 9.9 and an ionic strength μ = 444.4 mol/m^3 in the mixed product solution. Due to the limited stability of the reactants, both solutions were prepared directly before starting the experiments. After collecting the samples, the product mixture was diluted with buffer solution. The absorption of each sample was measured at a wavelength range of 400−700 nm. In order to determine the concentration of the different dyes, multilinear regression analysis was performed for the measured absorption spectra. The calculations with multilinear spectra are based on the molar extinction coefficients for each single substance given by Bourne and co-workers. Since the absorption spectra of the monoazo dyes are very similar, their concentrations were determined in sum ($c_{o\text{-}R} + c_{p\text{-}R}$).

Residence Time Distribution. Residence time behavior in the reactors was characterized by stimulus-response experiments. A step function in the tracer concentration was induced, while the outlet concentration profile was recorded using online UV−vis spectroscopy. Two feed streams, pure water and a 33 mg/L riboflavin tracer solution, were mixed at the reactor inlet. An automated procedure switches the flow ratio of both streams from 9:1 to 1:9 (and respectively vice versa). In order to determine possible adsorption of tracer molecules at the reactor wall, both step-up and step-down experiments were compared. The resulting *F*-curves appeared to be identical in very good approximation. Therefore, a possible retention and accumulation of tracer material in the reactor is negligible.

The dispersion model[12,13] was used for describing the residence time behavior in flow channels. Herein, the degree of back-mixing is expressed by the dimensionless Bodenstein number

$$\mathrm{Bo} = \frac{uL}{D_{ax}} \quad (3)$$

with the dispersion coefficient D_{ax}, which quantifies the effects of axial backmixing in one parameter. Applying eq 3, the *F*-curve given by Danckwerts[14] for open boundary conditions (i.e., no dispersion discontinuity) can be expressed as

$$F(\theta) = \frac{1}{2}\left[1 - \mathrm{erf}\left(\sqrt{\mathrm{Bo}}\,\frac{(1-\theta)}{\sqrt{4\theta}}\right)\right] \quad (4)$$

For determination of the Bo number, a least-square fit for the measured response signal curve was performed.

Scale-up Experiments. The experimental setup of the microreactor experiments was adapted for the use of a ceramic production reactor (Figure 2a, 3 M ESK Ceramics GmbH & Co KG, Germany) made from silicon carbide (SiC). Flow rates of 50 mL/min could be obtained with the same syringe pumps by using 25 mL syringes. In order to keep the reactor plates at constant temperature, a dynamic temperature control system (Tango, Huber GmbH, Germany) was employed. Temperature measurement at the reactor outlet was realized by using a T-junction in order to insert a Pt100 resistance thermometer (TMH GmbH, Germany) into the fluid channel (Figure 3).

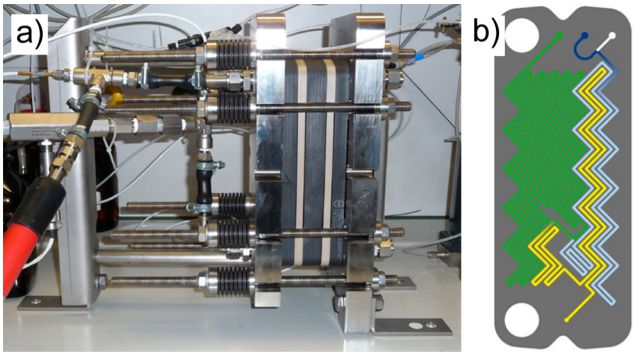

Figure 2. ESK ceramic production reactor (3M, Kempten) in the experimental setup (a) and plate design of the mixing module (b).

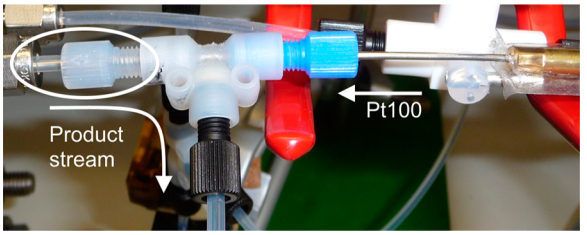

Figure 3. Temperature measurement in a capillary tube (inner diameter 2.4 mm) with a Pt100 sensor at the reactor outlet.

Thus, fluid flow encloses the entire measurement tip. Three different reactor modules, manufactured from silicon carbide, were used. A mixer module, including preheating channels, T-mixer, and a reaction channel (reaction volume, 2.9 mL), was combined with two residence time modules of 16.8 and 33.6 mL. The reaction channel with a square cross section (2.0 mm × 2.0 mm) is arranged in recurring 90° redirections (Figure 2b).

Since a flow rate of 50 mL/min would require an extremely high flow rate of quench solution, the quenching procedure had to be modified in order to use only part of the product stream for sampling and analysis. Therefore, a split-up of the product stream was realized by using a T-junction and a control valve to adjust the flow ratio. A Coriolis flow meter (mass flow meter M53, Bronkhorst High-Tech BV, The Netherlands) was used

dx.doi.org/10.1021/op5002758 | Org. Process Res. Dev. 2014, 18, 1535−1544

to determine the exact flow ratio between the main stream and the smaller stream for sampling (approximately 5 mL/min). Thus, the flow rate of quench solution could be adjusted to obtain the correct quench flow ratio of 10:1.

REACTOR CHARACTERISTICS

For kinetic studies, precise characterization of the reactor is crucial. When it comes to experimentally determining kinetic characteristics of a reaction, it is advantageous to keep approximately isothermal conditions and to use a reactor with low deviation from the ideal flow pattern, e.g., plug flow. Thus, kinetic parameters can be extracted from experimental data without taking into account complex physical processes such as back-mixing or the formation of local hot spots. Those deviations from the ideal isothermal plug flow behavior can cause a significant difference in the reaction progress. Therefore, preceding estimates should be performed in order to ensure that the reaction rate is decreased neither by a broad residence time distribution nor by reactant segregation due to poor mixing performance. Depending on the heat release of the reaction, heat removal in the reactor has to be fast enough to avoid a local hot spot at the entrance of the flow reactor.

The same criteria are important for scale-up considerations which are subject of this work. A scale-up toward higher flow rates is usually combined with an increase in the channel diameter. Residence time distribution strongly depends on the channel diameter, but also on channel design elements such as flow redirection, obstacles, or channel curvature. Mixing of larger flow rates might be a different task that requires a different mixing principle or higher energy input. A critical factor in scaling-up an exothermic reaction is the heat transfer. While microreactors have superior heat transfer characteristics, an increase in channel diameter causes not only a lower surface-to-volume ratio but also a lower heat transfer coefficient in the laminar flow. The fundamental equations that are the basis for choosing reactors and for the scale-up considerations in this work are discussed in the following. Detailed reviews about the design and characterization of microreactors can be found in literature.[15,16]

Residence Time Distribution. In order to determine the residence time distribution in a real flow reactor, the one-dimensional dispersion model was used. The material balance for a plug flow reactor in steady state is extended by an additional term that describes axial dispersion with the dispersion coefficient D_{ax}. For a component j, it can be written as

$$D_{ax}\frac{\partial^2 c_j}{\partial z^2} - u\frac{\partial c_j}{\partial z} + \nu_j r = 0 \tag{5}$$

The dispersion coefficient D_{ax} combines the effects of backmixing due to a radial velocity profile in laminar flow, molecular diffusion, and the formation of secondary flow in one parameter.

For laminar flow in empty tubes with circular cross-section, D_{ax} can be determined as a function of the molecular diffusivity D_m, using the correlation of Taylor[17] and Aris:[18]

$$D_{ax} = D_m + \frac{u^2 d_t^2}{192 D_m} \tag{6}$$

Low axial dispersion in straight microchannels with laminar flow is only possible if there is enough time for a diffusive compensation of the radial concentration differences, which are caused by the laminar velocity profile. Therefore, in order to obtain lower axial diffusion and a higher Bo number (see eq 3), it is necessary to increase the time ratio τ/t_D with the hydrodynamic residence time τ and the characteristic time for molecular diffusion $t_D = d_t^2/D_m$. In other words, the shorter the mean residence time in the reactor, the smaller is the required diameter to obtain a high Bo number.

As stated above, two different capillary reactors were chosen. For short reaction times, a stainless steel capillary reactor (MR1) with an inner diameter of 250 μm is used. For high mean residence times in a 250 μm channel, either an extremely low flow rate or an extremely long reactor channel is required, which would cause a very high pressure drop. Both possibilities are limited by the specifications of the employed syringe pumps. Hence, higher residence times were realized in a second capillary reactor (MR2) with a larger inner diameter of 750 μm. Due to the longer residence times, similar Bo numbers can be obtained for similar flow rates in both microreactors.

For a further increase of the Bo number, the capillary reactor is helically coiled with a radius of curvature of 8 mm. The centrifugal force causes a secondary flow in form of inversely rotating vortices. A measure for the strength of these secondary flows is the Dean number

$$\mathrm{Dn} = \mathrm{Re}(d_t/2R)^{1/2} \tag{7}$$

The work of Janssen on axial dispersion in coiled tubes[19] showed that dispersion can be correlated by the dimensionless parameter $\mathrm{Dn}^2\mathrm{Sc}$, where the Schmidt number Sc is given by $\mathrm{Sc} = \eta/(\rho D_m)$. A significant reduction of axial dispersion compared to the Taylor–Aris prediction for a straight tube is predicted for $\mathrm{Dn}^2\mathrm{Sc} > 200$. In contrast to common helically coiled reactors, the capillary is coiled with an alternating change in the direction of curvature, which is repeated every two coils. Preliminary experiments for the residence time showed a small decrease in axial dispersion compared to a uniformly coiled helix.

Table 1 compares both microreactors used for kinetic investigation of the Michael addition. The dimensionless parameters Re, Dn, and Bo vary with the applied flow rate. They were exemplarily calculated for aimed mean residence times, chosen in order to obtain low conversions in reactor MR1 and high conversions in reactor MR2. The Bo number according to Janssen,[19] taking into account the secondary flow, is increased by a factor of about 3 in comparison with the Taylor–Aris correlation for straight tubes. This is in good agreement with our own experiments and recently published

Table 1. Channel dimensions of the microreactors used for the kinetic study and dimensionless parameters, calculated for selected mean residence times

reactor		MR1	MR2
channel diameter	(mm)	0.25	0.75
length	(m)	0.50	0.50
inner volume	(mL)	0.025	0.221
mean residence time	(s)	**5**	**60**
flow rate	(mL/min)	0.29	0.22
flow velocity	(m/s)	0.10	0.008
Re number		21.6	5.4
Dn number		2.70	1.17
Bo number (Taylor–Aris)		15	21
Bo number (Janssen)		51	58

dx.doi.org/10.1021/op5002758 | Org. Process Res. Dev. 2014, 18, 1535–1544

experimental data.[20] For high Bo numbers, the dispersion term in eq 5 can be neglected in good approximation. The common threshold for the assumption of plug flow conditions is a value of Bo > 100.[13] However, this threshold is not a sharp boundary. The effect of the residence time distribution on the reaction progress not only is a function of the Bo number, but also depends on reaction kinetics and the conversion obtained in the reactor. For Bo numbers less than 100, the influence of axial dispersion can be calculated by applying eq 5. This approach was performed for the conditions summarized in Table 1. With the reaction kinetics of the Michael addition and Bo numbers in the range of 50, a conversion decrease of less than 1% is the result of the deviation from ideal plug flow behavior. Hence, application of the plug flow assumption can be considered as justified in good approximation. Further results and details of the calculation can be found in the Supporting Information.

Mixing. For a kinetic study, the determined reaction rate should not be influenced by the mixing process. Thus, the main objective in mixing is to achieve short mixing times compared to the time of chemical reaction. In every mixing process, molecular diffusion is required as the final step, when it comes to mixing reactants on a molecular scale. A suitable micromixer is able to reduce the length scale of diffusion. For this purpose, several types of micromixers exist. In a previous paper,[21] an experimental approach has been carried out to characterize mixing performance with competitive reaction systems. For low flow rates (< 10 mL/min), the best mixing performance was found for a slit interdigital mixer (SIMM, Fraunhofer ICT-IMM, Mainz, Germany). It can be assumed that this is due to the formation of multilamellae flow smaller than 100 μm in microstructures. Therefore, short diffusion paths are generated.

For the kinetic experiments at low flow rates, the SIMM was chosen in combination with the reactor capillaries MR1 and MR2. Considering a scale-up to higher reactor throughputs, this mixer type is not transferable due to the high pressure drop in the microstructured device. A different mixing principle has to be found with comparable mixing performance at high flow rates.

Heat Removal. The objective to run the reaction at approximately isothermal conditions can be achieved if heat removal in the reactor is high in comparison with the generation of heat by the reaction. While the released heat of reaction changes due to concentration decrease as the reaction progresses, heat removal depends on the local temperature of the reaction mixture. For this reason, it is difficult to estimate the temperature profile in a reactor without exact kinetic data. However, for a rough estimation, the expected time for reaction t_R can be compared to the characteristic time for heat transfer.[22]

$$t_h = \frac{\rho c_p d_t}{4\alpha} \tag{8}$$

With the assumption of a constant wall temperature, heat transfer in laminar flow is characterized by the constant Nußelt number[23]

$$\mathrm{Nu} = \frac{\alpha d_t}{\lambda_f} = 3.66 \tag{9}$$

Using eq 9 to calculate the heat transfer coefficient α shows that an increase in the channel diameter d_t by 1 order of magnitude extends the characteristic time for heat exchange by 2 orders of magnitude. The reactor design for an exothermic reaction should ensure a comparatively short time for cooling ($t_h \ll t_R$). Table 2 shows the heat transfer parameters for the reactors MR1 and MR2. Due to the smaller channel diameter, the specific surface area and the heat transfer coefficient in MR1 are three times larger than in MR2. As a result, the characteristic time for heat transfer differs by a factor of 9. However, heat transfer parameters indicate very efficient heat removal for both microreactors, even for fast exothermic reactions (10 s < t_R < 10 min).

Table 2. Characteristic parameters for heat transfer in the investigated microreactors

reactor		MR1	MR2
channel diameter	(mm)	0.25	0.75
specific surface area	(m^2/m^3)	16 000	5333
heat transfer coefficient α	($W/(m^2K)$)	2194	731
transfer time t_h	(s)	0.030	0.273

If kinetic data are available, the temperature profile in a plug flow reactor can be calculated by using the energy balance

$$\rho u c_p \frac{\mathrm{d}T}{\mathrm{d}z} + r\Delta H_R + k\frac{4}{d_t}(T - T_W) = 0 \tag{10}$$

With the reaction rate r as a function of the reactant concentration, this equation is coupled with the material balance (eq 5). It was assumed that the overall heat transfer coefficient k is mainly is determined by the coefficient of heat transfer α in the reaction channel. Heat transfer in the oil bath and heat conduction in the wall of the stainless steel capillary is considered to be very high in relation to the inner heat transfer.

REACTION KINETICS OF THE MICHAEL ADDITION

A lot of aza-Michael reactions with amines can be performed easily at ambient temperature and without any catalyst.[24] Some of them seem to follow second-order kinetics based on the concentrations of the nucleophile (amine) and the Michael acceptor.[25] However, in the case of the chosen reaction with piperidine and ethyl acrylate, a simple second order mechanism did fit the experimental data only by rough estimation. In consequence, a more detailed kinetic model had to be chosen. As shown in Scheme 2, a zwitterionic intermediate is formed by the nucleophilic attack on the activated double bond.

The precise mechanism of the subsequent proton transfer towards the neutral product is unknown, but can be considered as a bottleneck in the reaction mechanism. In literature, a direct intramolecular transport is reported as well as a solvent or reactant-assisted proton transfer.[26] A publication about the mechanism of the addition of amines to trans-(2-furyl)-nitroethylene[27] demonstrates that this reaction is catalyzed by a second molecule of the amine reactant. For the aza-Michael reaction, a recent publication describes significant rate acceleration for the addition in the presence of water.[28] Both observations lead to the conclusion that a water molecule as well as an amine molecule can act as shuttle for the proton and therefore promotes the charge equalization of the zwitterionic intermediate.

In the experimental work, these dependencies of reaction rate could be confirmed for the current Michael addition. A reaction kinetic that is second order in the piperidine and first order in ethyl acrylate was suitable to describe the conversion as reaction progresses with increasing residence time. Furthermore, a strong influence of water as catalyst could be observed. An addition of 0.25 equiv of water doubles the reaction rate,

dx.doi.org/10.1021/op5002758 | Org. Process Res. Dev. 2014, 18, 1535−1544

Scheme 2. Formation of a zwitterionic intermediate in the Michael addition

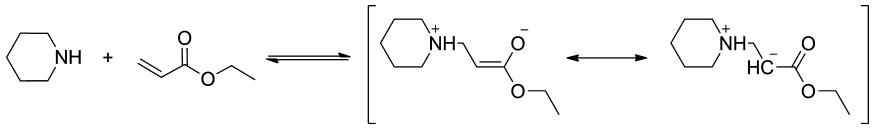

Scheme 3. Assumed reaction scheme for kinetic modelling

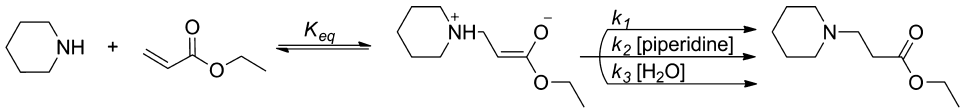

and a linear dependency between water addition and reaction rate seems to exist. In order to describe all experimental data with a kinetic model, Scheme 3 were used as a basis for a data fitting with the software DynoChem (Scale-up Systems Ltd., Ireland). This model includes the unassisted, water-assisted, and amine-assisted proton transfer.

As a result of the fitting, the rate constant k_1 tends to zero; thus the unassisted pathway can be neglected at least in the case of an undiluted reaction mixture. Assuming a rapid equilibration towards the intermediate, the concentration of the intermediate can be described as

$$c_{\mathrm{Int}} = K_{\mathrm{eq}} c_{\mathrm{Pip}} c_{\mathrm{EA}} \tag{11}$$

which leads to a total rate expression of

$$r = k_3 K_{\mathrm{eq}} c_{\mathrm{Pip}} c_{\mathrm{EA}} c_{\mathrm{H_2O}} + k_2 K_{\mathrm{eq}} c_{\mathrm{Pip}}^2 c_{\mathrm{EA}} \tag{12}$$

Using the observed rate constants $k_{\mathrm{obs,A}} = k_2 K_{\mathrm{eq}}$ and $k_{\mathrm{obs,B}} = k_3 K_{\mathrm{eq}}$, the reaction scheme can be simplified with two parallel reactions (Scheme 4).

Scheme 4. Simpified reaction scheme for kinetic modelling

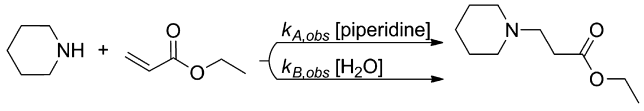

Figure 4 shows fitted curves for both considered mechanisms. The deviations between the observed rate constants in Scheme 4 and the products $k_2 K_{\mathrm{eq}}$ and $k_3 K_{\mathrm{eq}}$ (Scheme 3) are below 3%. For both mechanisms fittings are based on 120 data points. Conversion curves were determined for different temperatures (30−70 °C), different amounts of water addition (0−1.05 equiv H_2O), and different molar ratios of reactants (1.01−1.22 equiv piperidine).

All experimental data could be described in good approximation by using the simplified reaction scheme. The difference between the fitting based on Scheme 3 and Scheme 4 is shown in Figure 4 for different stoichiometric ratios. Acceleration of the reaction by increasing the amine ratio is obvious and in agreement with the considered mechanism. Furthermore, the strong influence of water, as demonstrated in Figure 5, can also be described well by the kinetic model.

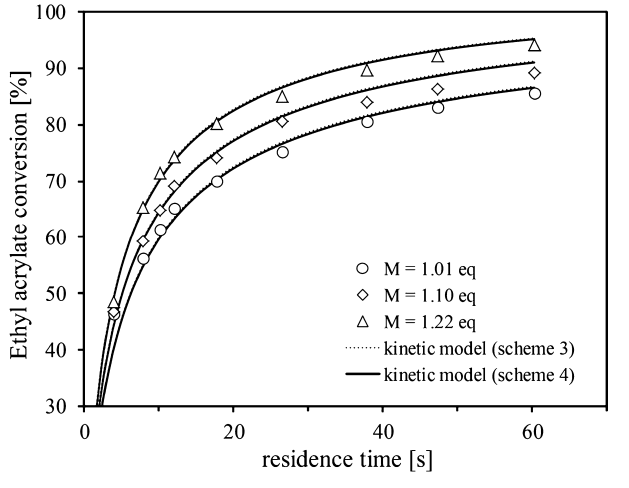

Figure 4. Comparison of a curve fitting using both kinetic models ($c_{\mathrm{EA,0}}$ = 4 mol/L, T = 30 °C, W = 0.25 equiv).

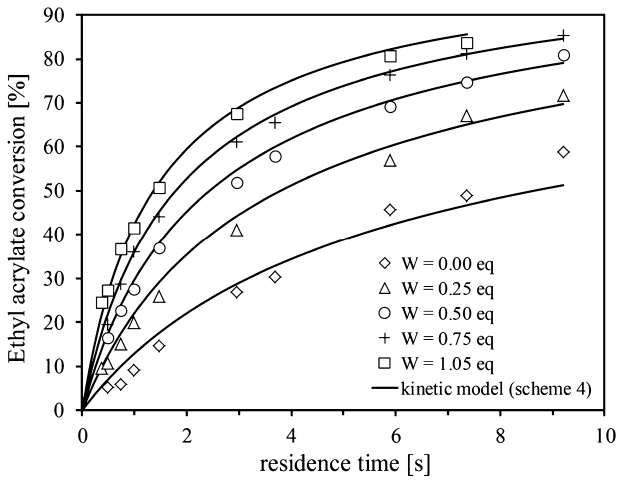

Figure 5. Kinetic model and experimental data for different amounts of water addition ($c_{\mathrm{EA,0}}$ = 4 mol/L, T = 30 °C, M = 1.1 equiv).

In the simplified reaction scheme, fitting parameters are reduced to the observed third order rate constants $k_{\mathrm{obs,A}}$ and $k_{\mathrm{obs,B}}$ and the observed activation energies $E_{\mathrm{A,obs,A}}$ and $E_{\mathrm{A,obs,B}}$. The temperature dependency of both observed rate constants was surprisingly low; the activation energies $E_{\mathrm{A,obs,A}}$ = 0 kJ/mol and $E_{\mathrm{A,obs,B}}$ = 14 kJ/mol resulted from the curve fitting (Figure 6). In general, activation energies that are close to zero often indicate mass transfer limitations. Since reaction takes place in an efficiently mixed, single-phase flow, mass transfer limitation can be neglected. Furthermore, low temperature dependency can be accounted for by the presence of an exothermic pre-equilibrium step in the reaction mechanism, which again would be in good agreement with the proposed mechanism in Scheme 3. In this case, the observed activation energy would be the sum of the actual activation energy and the standard enthalpy of

dx.doi.org/10.1021/op5002758 | Org. Process Res. Dev. 2014, 18, 1535−1544

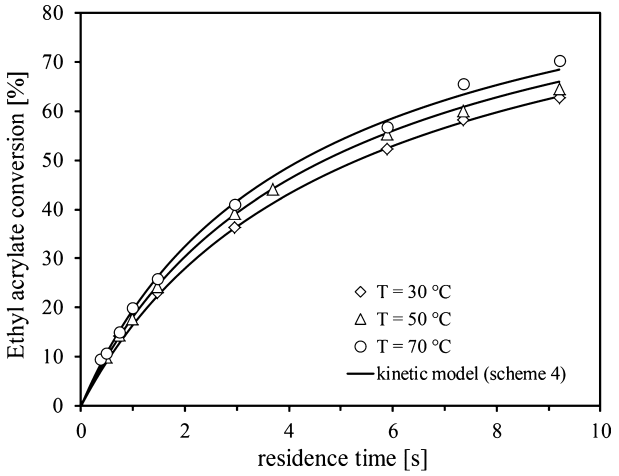

Figure 6. Kinetic model and experimental data for different reactor temperatures ($c_{EA,0}$ = 4 mol/L, M = 1.1 equiv, W = 0.25 equiv).

reaction, which describes the temperature dependency of the equilibrium step.[29]

$$E_{A,obs} = E_A + \Delta H_R^0 \quad (13)$$

A derivation of this correlation can be found in the Supporting Information.

SCALE-UP OF REACTOR CONCEPT

Capillary reactors with specific length, inner diameter, and curvature are very flexible and easy to implement in small-scale microreactor setups for kinetic experiments. In order to maintain flexibility in production scale reactors, modular plate reactors provide a suitable reactor concept. Process and utility channels in the reactor modules of the ESK production reactor can be combined to achieve a reactor with the required inner volume. The considered scale-up not only implies a transfer of channel dimensions, but also a change of flow guidance, channel cross-section, and mixing principle. Since a different reactor behavior can be expected, mass and heat transfer processes have to be characterized experimentally. A set of preliminary experiments for characterization is proposed, and the results are discussed in the following.

Residence Time Distribution. As discussed above, in strictly laminar flow, back-mixing mainly depends on the mean residence time in relation to the characteristic time for molecular diffusion. Considering the scale-up to larger channel dimensions in the ESK reactor, the time for molecular diffusion would increase quadratically with the channel width. If radial mass transport is only based on molecular diffusion, this would result in a broad residence time distribution with an equivalent decrease in the Bo number. However, the channel design of the reactor can induce secondary flow structures which significantly support the radial mass transport. In the ESK reactor, repeated alternating 90°-redirections enhance the homogenization of the radial concentration profile in the laminar flow. The resulting residence time behavior was determined experimentally by stimulus-response experiments.

Figure 7 shows the residence time function that is obtained from the response signal of an automatically induced step function of the tracer concentration. A numerical fit of the dispersed plug flow model was performed, with Bo as the only fitting parameter. The best fit for the dispersion model was obtained with a Bo number of 1130. This result indicates

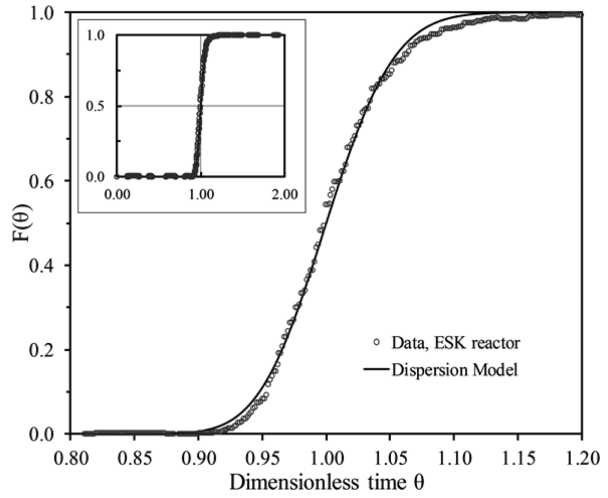

Figure 7. Measured F-function and model fits for the ESK production reactor at a total flow rate of 50 mL/min.

surprisingly low axial dispersion, and as a consequence, plug flow behavior can be assumed in very good approximation. Since a narrow residence time distribution was determined for the considered length scales of all reactors, eq 5 can be simplified by neglecting the dispersion term.

The measurements in the ESK reactor demonstrate the fact that 90° bends in the reactor channel can be considered as efficient mixing elements, which induce secondary flow structures. Faster fluid from the middle of the channel is forced to the outer wall due to centrifugal forces. This effect strongly depends on the Reynolds number Re. As described in literature,[15] the present Re number (Re ≈ 300 at a flow rate of 50 mL/min) is sufficiently high to induce a pronounced secondary flow structure in each 90° bend (L-mixer).

Mixing. The mixing zone in the SiC reactor module of the ESK production reactor is a T-mixer with 2 mm channel width. Reactants are contacted and redirected with 90° into the reaction channel. As described above, mixing sensitive test reactions were used as a practical approach to estimate the mixing performance. Figure 8 shows the results of the fourth Bourne test reaction for different flow rates. A low yield of the bisazo dye indicates a short mixing time that is below the

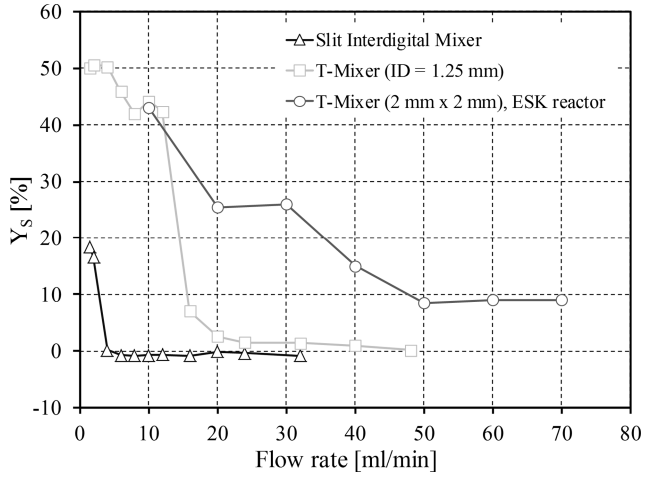

Figure 8. Experimental results of the fourth Bourne test reaction for the investigated mixer types.

dx.doi.org/10.1021/op5002758 | Org. Process Res. Dev. 2014, 18, 1535−1544

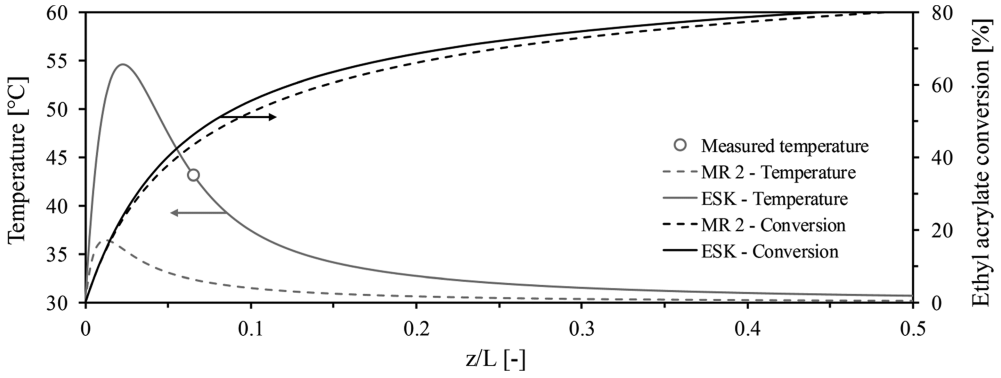

Figure 9. Simulation of conversion and temperature in the reaction channel of the ESK flow reactor, compared with the microreactor MR2.

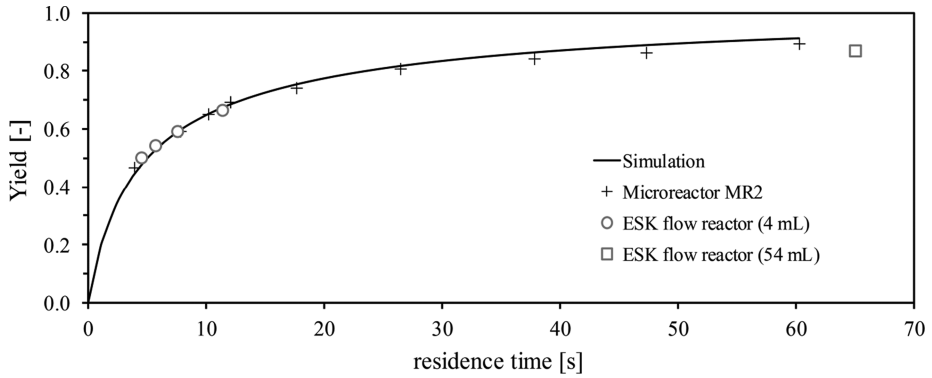

Figure 10. Kinetic model and experimentally determined yields in the microreactor and in the ESK ceramic production reactor.

reaction time of about 800 ms. Measurements with the ESK reactor are compared to results of a previous study[21] for the slit interdigital mixer and a T-mixer with circular cross-section and 1.25 mm inner diameter.

In every micromixer, the final step in mixing is an equalization of fluid lamellae by molecular diffusion. In the slit interdigital mixer, these fluid lamellae are mainly created by the multilamination mixing principle. In contrast, in a T-shaped mixer convective mixing induces secondary flow structures with small fluid lamellae. Therefore, a significantly higher flow velocity is needed in the T-mixer in order to obtain similar mixing times for both types of micromixer. Mixing behavior of T-mixers is well-described in literature.[15] Since the mixing performance depends on the Re number, a larger channel diameter has to be compensated by a higher flow rate. Figure 8 shows that, in the ESK production reactor, a minimum flow rate of about 20 mL/min is required to ensure a mixing time comparable to the mixing time in the SIMM at very low flow rates. Hence, the convective mixing principle of a T-junction provides a high efficiency in the employed reactor modules at the aimed production rate of 50 mL/min. In contrast, however, a T-mixer would not be suitable for the previously described kinetic experiments in a small scale microreactor.

Heat Removal. In the bonded reactor plates of the ceramic production reactor, it is not possible to measure temperatures inside the reaction channel. For this reason, the location and extent of the hot spot have to be estimated by simulations. Assuming that the reaction rate as well as the heat transfer in the reactor can be described with good accuracy, eq 10 allows for calculation of the temperature profile in the reactors. Due to the kinetic experiments, the reaction heat source is known as a function of concentration and temperature. First approximations for the heat transfer coefficient in straight laminar flow (Table 2) demonstrated the general problem of the scale-up to larger channel widths due to the quadratic dependency of the heat transfer coefficient. However, it can be assumed that secondary flow in the reaction channel enhances the heat transfer. The calculated coefficient for straight laminar flow would underestimate the actual value which is influenced by the flow velocity and secondary flow formation. Therefore, the *k*-value is an unknown parameter in eq 10.

A measurement of the temperature at the outlet of the first reactor plate showed a temperature difference of 13 K compared to the oil temperature in the reactor plate. This measurement was used to perform a fitting of the temperature profiles by adjusting the heat transfer coefficient (Figure 9). While the calculation for straight laminar flow, based on eq 9, results in a heat transfer coefficient of 274 W/(m^2·K), the fitting method leads to a result of 500 W/(m^2·K). Thus, the comparison indicates a significant enhancement in heat transfer caused by the flow guidance in the reactor channel. However, the hot spot is still about 5 times larger compared to the micromixer, and a temperature rise of 25 degrees could be critical for reaction control. In the case of the Michael addition, the influence of the hot spot in the production reactor is predicted to be extremely small. As can be seen in Figure 9, only a slight acceleration of the reaction rate in the entrance region of the reaction channel can be predicted compared to the nearly isothermal microreactor. This result can be explained by the exceptional low activation energy of the Michael addition. As the kinetic experiments showed, no side reaction should be expected in the overheated regions of the reactor. Nevertheless, it is still important to estimate the hot spot for

dx.doi.org/10.1021/op5002758 | Org. Process Res. Dev. 2014, 18, 1535−1544

the production scale reaction process, in order to avoid decomposition or boiling of the reaction mixture.

Scale-up Verification. The combination of preliminary experiments and simulations made it possible to predict the reaction yield in the examined production reactor under various reaction conditions. Two types of experiment were performed in order to verify the scale-up considerations. First, a reactor setup with the mixing module (4 mL internal volume) and without further residence time modules was used to examine the reaction progress at short reaction times. The total flow rate was kept constant at 50 mL/min and subsequently reduced stepwise down to 20 mL/min in order to get four data points at the steep beginning of the yield−time curve. A further decrease of the flow rate would not be practical, since the mixing efficiency in the T-mixer would decrease significantly (Figure 8). In a second experiment, the operation point was chosen in order to reach a yield of about 90% in a long-term operation at the aimed production rate of 50 mL/min. Steady state conditions were obtained after about 20 min of operation. A constant yield of 87% at the reactor outlet was determined by GC analysis, which is slightly lower than the predicted yield (90%). A limit in residence time is given by the total volume of the three available reactor modules (54 mL). In order to reach higher conversions, further residence time modules could be added to the reactor setup. In Figure 10, the results of both experiments are shown in comparison with the simulated curve. Excellent agreement of the calculated and measured conversion confirms the prediction that neither a broad residence time distribution nor a bad mixing performance influences the reaction progress significantly.

Results from the microreactor experiment with comparable reaction conditions confirm the simulation results presented in Figure 9: Despite the different temperature profiles, the reaction rate is very similar in both reactors. No influence of the pronounced hot spot in the production reactor was observed, and the measured temperature and outlet concentrations prove stable reactor control. It must, however, be emphasized that low temperature dependence is unusual for chemical reactions and a specific characteristic of the examined Michael addition. In contrast, assuming an arbitrary exothermic reaction with higher activation energy, runaway behavior, and parametric sensitivity can limit the operability of the reactor. Scale-up considerations should then be extended by correlations, which predict the limit of reaction runaway (e.g., Semenov model, Barkelew−Renken approach).[30,31] As a consequence, it could be necessary to consider alternative reactor designs, e.g., multi-injection reactors[32,33] or a successive enlargement of the reaction channel in order to combine heat control in the mixing zone with high-volume residence time modules.[34,35]

CONCLUSIONS

Several steps of process development in flow chemistry have been discussed in this contribution, using the Michael addition of piperidine to ethyl acrylate as an example. A systematic approach for the transfer of lab experiments in microstructured devices to the conditions of small-scale production processes is proposed. Preliminary calculations, which focus on characteristic times of transport phenomena, can be used in order to ensure the operability of the production scale reactor. Further experiments for reactor characterization provide additional information to describe mixing, residence time distribution, and heat transfer in the examined reactors. Therefore, geometric similarity is not necessary in this scale-up approach, regarding both mixer and channel design. Using the one-dimensional dispersed plug-flow model, conversion and temperature profiles can be simulated by correlating the reaction kinetics with transport mechanisms. Applying this simplified reactor model, based on results of lab experiments, is a suitable approach for the prediction of scale-up effects. In the case of strong axial dispersion (low Bo numbers) or uncontrollable hot spots, the simulation would indicate the scale-up limitations. Application of the systematic scale-up approach made it possible to perform a valid transfer of the reaction to the ESK production reactor.

Plug flow behavior as well as short mixing times compared to reaction time could be obtained for all employed reactors. In case of exothermic reactions, insufficient heat transfer has to be considered as a crucial scale-up issue. Therefore, hot spots were located by correlating reaction kinetics and heat transfer in the reactor channel. It was shown that even though pronounced hot spots occur in the ESK production reactor, they do not affect the reaction control of the Michael addition with low activation energy.

ASSOCIATED CONTENT

Supporting Information

A closer look at the influence of axial dispersion in the microreactors that were used for the kinetic studies; derivation of eq 13. This material is available free of charge via the Internet at http://pubs.acs.org.

AUTHOR INFORMATION

Corresponding Author

* E-mail: t.roeder@hs-mannheim.de. Telephone: +49 621 292 6800.

Notes

The authors declare no competing financial interest.

ACKNOWLEDGMENTS

This work was funded by the German Federal Ministry of Education and Research (BMBF, funding code 03FH012I2). The authors would like to thank Jürgen Sprinz and Andreas Zietsch (CHESS GmbH, D-68169 Mannheim, Germany) for valuable discussions, and Scale-up Systems Ltd. (Dublin 4, Ireland) for providing the software DynoChem.

NOTATIONS

Bo	Bodenstein number
c_j	concentration of component j (mol m^{-3})
$c_{j,0}$	theoretical, initial concentration of component j in the reaction mixture (mol m^{-3})
c_p	heat capacity (J kg^{-1} K^{-1})
d_t	hydraulic channel/tube diameter (m)
D_{ax}	axial dispersion coefficient (m^2 s^{-1})
D_m	molecular diffusion coefficient (m^2 s^{-1})
Dn	Dean number
$E_{A,i}$	activation energy of reaction i (J mol^{-1})
$E_{A,obs,i}$	observed activation energy of reaction i (J mol^{-1})
erf(x)	$(2/\sqrt{\pi})\int_0^x e^{-t^2}\,dt$
$F(\theta)$	dimensionless integral distribution function
ΔH_R^0	standard enthalpy of reaction (J mol^{-1})
k	overall heat transfer coefficient (W m^{-2} K^{-1})
k_i	rate constant of reaction i, n-th order (L^{n-1} mol^{1-n} s^{-1})
$k_{obs,i}$	observed rate constant of reaction i, n-th order (L^{n-1} mol^{1-n} s^{-1})

K_{eq} equilibrium constant
L channel length (m)
M molar ratio of reactants $c_{Pip,0}/c_{EA,0}$
Nu Nußelt number
r reaction rate (mol L^{-1} s^{-1})
R radius of curvature (m)
Re Reynolds number
Sc Schmidt number
t time (s)
$\overline{t}$ mean residence time (s)
t_D characteristic time scale of molecular diffusion (s)
t_h characteristic time scale of heat transfer (s)
t_R characteristic time scale of reaction (s)
T temperature (K)
T_W temperature at the wall (K)
u mean fluid velocity (m s^{-1})
W molar ratio of water addition $c_{H_2O,0}/c_{EA,0}$
X_j conversion of component j
Y_S yield of product S
z channel length coordinate (m)

Greek Symbols

α heat transfer coefficient (W m^{-2} K^{-1})
η dynamic viscosity (N s m^{-2})
θ time, nondimensionalized with $\overline{t}$
λ_f heat conductivity of the fluid (W m^{-1} K^{-1})
μ ionic strength (mol m^{-3})
ν_j stoichiometric coefficient of component j
ρ density (kg m^{-3})
τ hydrodynamic residence time (s)

REFERENCES

(1) Hessel, V.; Kralisch, D.; Kockmann, N.; Noël, T.; Wang, Q. *ChemSusChem* **2013**, *6* (5), 746−789.
(2) Yoshida, J.-i.; Nagaki, A.; Yamada, T. *Chem.—Eur. J.* **2008**, *14* (25), 7450−7459.
(3) Falk, L.; Commenge, J. M. *Chem. Eng. Sci.* **2010**, *65* (1), 405−411.
(4) Saber, M.; Commenge, J. M.; Falk, L. *Chem. Eng. Sci.* **2010**, *65* (1), 372−379.
(5) Tonomura, O.; Tominari, T.; Kano, M.; Hasebe, S. *Chem. Eng. J.* **2008**, *135*, 131−137.
(6) Kockmann, N.; Gottsponer, M.; Roberge, D. M. *Chem. Eng. J.* **2011**, *167* (2−3), 718−726.
(7) Löwe, H.; Hessel, V.; Löb, P.; Hubbard, S. *Org. Process Res. Dev.* **2006**, *10* (6), 1144−1152.
(8) Lerou, J. J.; Tonkovich, A. L.; Silva, L.; Perry, S.; McDaniel, J. *Chem. Eng. Sci.* **2010**, *65* (1), 380−385.
(9) Bourne, J. R.; Kut, O. M.; Lenzner, J.; Maire, H. *Ind. Eng. Chem. Res.* **1990**, *29* (9), 1761−1765.
(10) Baldyga, J.; Bourne, J. R.; Walker, B. *Can. J. Chem. Eng.* **1998**, *76* (3), 641−649.
(11) Baldyga, J.; Bourne, J. R. *Turbulent mixing and chemical reactions*; Wiley: New York, 1999.
(12) Westerterp, K. R.; van Swaaij, W. P. M.; Beenackers, A. A. C. M.; Kramers, H. *Chemical reactor design and operation*; Wiley: Chichester, Sussex, 1984.
(13) Levenspiel, O. *Chemical reaction engineering*; Wiley: New York, 1999.
(14) Danckwerts, P. V. *Chem. Eng. Sci.* **1953**, *2* (1), 1−13.
(15) Kockmann, N. *Transport phenomena in micro process engineering: Fundamentals, devices, fabrication, and applications*; Springer: Berlin, 2008.
(16) Hessel, V.; Renken, A.; Schouten, J. C.; Yoshida, J.-i. *Micro Process Engineering*; Wiley-VCH: Weinheim, 2009.
(17) Taylor, G. *P. R. Soc. London A Mater.* **1953**, *219* (1137), 186−203.
(18) Aris, R. *P. R. Soc. London A Mater.* **1956**, *235* (1200), 67−77.
(19) Janssen, L. *Chem. Eng. Sci.* **1976**, *31* (3), 215−218.
(20) Minnich, C. B.; Sipeer, F.; Greiner, L.; Liauw, M. A. *Ind. Eng. Chem. Res.* **2010**, *49* (12), 5530−5535.
(21) Schwolow, S.; Hollmann, J.; Schenkel, B.; Röder, T. *Org. Process Res. Dev.* **2012**, *16* (9), 1513−1522.
(22) Kockmann, N.; Gottsponer, M.; Zimmermann, B.; Roberge, D. M. *Chem.—Eur. J.* **2008**, *14* (25), 7470−7477.
(23) Marek, R.; Nitsche, K. *Praxis der Wärmeübertragung*; Carl Hanser Verlag GmbH: München, 2007
(24) Ranu, B. C.; Dey, S. S.; Hajra, A. *Arkivoc* **2002**, *7*, 76−81.
(25) Mather, B. D.; Viswanathan, K.; Miller, K. M.; Long, T. E. *Prog. Polym. Sci.* **2006**, *31* (5), 487−531.
(26) Pardo, L.; Osman, R.; Weinstein, H.; Rabinowitz, J. R. *J. Am. Chem. Soc.* **1993**, *115* (18), 8263−8269.
(27) Popov, A. F.; Perepichka, I. F.; Kostenko, L. I. *J. Chem. Soc., Perkin Trans. 2* **1989**, No. 5, 395.
(28) Ranu, B. C.; Banerjee, S. *Tetrahedron Lett.* **2007**, *48* (1), 141−143.
(29) Wedler, G. *Lehrbuch der physikalischen Chemie*; VCH: Weinheim, 1987.
(30) Baerns, M. *Technische Chemie: Das Lehrbuch*; Wiley-VCH: Weinheim, 2006.
(31) Kockmann, N. *Chem. Ing. Technol.* **2012**, *84* (5), 715−726.
(32) Barthe, P.; Guermeur, C.; Lobet, O.; Moreno, M.; Woehl, P.; Roberge, D. M.; Bieler, N.; Zimmermann, B. *Chem. Eng. Technol.* **2008**, *31* (8), 1146−1154.
(33) Haber, J.; Kashid, M. N.; Renken, A.; Kiwi-Minsker, L. *Ind. Eng. Chem. Res.* **2012**, *51* (4), 1474−1489.
(34) Waterkamp, D. A.; Heiland, M.; Schlüter, M.; Sauvageau, J. C.; Beyersdorff, T.; Thöming, J. *Green Chem.* **2007**, *9* (10), 1084.
(35) Renken, A.; Hessel, V.; Löb, P.; Miszczuk, R.; Uerdingen, M.; Kiwi-Minsker, L. *Chem. Eng. Process.* **2007**, *46* (9), 840−845.